Available online at www.sciencedirect.com
ScienceDirect
Journal of Molecular Catalysis B: Enzymatic 43 (2006) 44–48
JOURNAL OF MOLECULAR CATALYSIS B: ENZYMATIC
www.elsevier.com/locate/molcatb

Visible-light photocatalytic regeneration of NADH using P-doped TiO_2 nanoparticles

Qing Shi, Dong Yang, Zhongyi Jiang *, Jian Li

School of Chemical Engineering and Technology, Tianjin University, Tianjin 300072, PR China

Available online 1 August 2006

Abstract

P-doped TiO_2 nanoparticles were prepared by the sol–gel method and characterized by XRD, BET, SEM, XPS and UV–vis spectrum. The results indicated that the doping of phosphorus could efficiently inhibit the grain growth and enhance the surface area of TiO_2 nanoparticles. The doped phosphorus was present as the pentavalent-oxidation state, which can replace a part of Ti^{4+} in the crystal lattice of anatase. Because P^{5+} can accept photoelectron as the electron trap center, its doping reduces the recombination rate of photogenerated charge carriers. In addition, P-doped TiO_2 nanoparticles also show stronger absorption in the visible light range than the pure sample, because of the formation of an impurity energy level within the band gap of TiO_2. Correspondingly, P-doped TiO_2 nanomaterials show higher ability of NADH photogenenration under visible-light irradiation than pure TiO_2.
© 2006 Elsevier B.V. All rights reserved.

Keywords: TiO_2; NADH; Phosphorus; Doping; Photocatalyse

1. Introduction

In the past two decades, the application of enzymes has grown rapidly in the chemical, food and pharmaceutical industry field, because most of them operates under benign aqueous conditions and at room temperature, accepts a wide range of complex molecules as substrates, and has exquisite enantio- and region-selectivity [1,2]. Compared with the enzymes used as the sole catalyst in a reaction, a number of cofactor-dependent enzymes such as oxidoreductases and transferases, are able to catalyze more complex and synthetically useful chemistry reaction, the costly nature of which precludes their use as stoichiometric reagents. Therefore, the continuous regeneration of cofactors *in vitro* attracts growing research interest in recent years [3]. In addition to reducing the cost, the cofactor regeneration can also drive the reaction to completion, prevent the accumulation of inhibitory cofactor by-products, simplify product isolation and increase enantio-selectivity.

Nicotinamide adenine dinucleotide (NADH) [4] is one of the most important cofactors in the biosynthesis involving many oxidoreductases. To date, a number of strategies including enzymatic catalysis [5–7], whole-cell conversion [8–10], chemical method [11–14], have been devised to the regeneration of NADH. Among these, photochemical method [15–19] attracts more attention because of the efficient utilization of clean and cheap solar energy. In the photochemical process of NADH regeneration, the photosensitizer acts the important roles, which usually uses dispersed semiconductor materials, such as TiO_2 and CdS particles, or multilayer TiO_2 film. However, TiO_2 has a wide band gap (3.2 eV) and can only be excited by ultraviolet light less than 387 nm, which accounts for about 2–3% of sun's energy [20,21]. Though CdS is a narrow band semiconductor, it corrupts under photo irradiation. Thus, a challenge for the photochemical regeneration of NADH is to find the stable visible-light photosensitizer.

Much effort including doping of transition metal ions [22–26] and nonmetallic anions [27–30], coupling with small bandgap semiconductors [31–34], and sensitization with dyes, etc. [35,36], have been employed to extend the light absorption of titanium dioxide to the visible region. It is noteworthy that phosphorous species attract increasing interest recently because of their ability to stabilize mesoporous structures and desired ability to enhance the photocatalytic activity [37–39]. For example, Yu et al. [37] found that direct incorporation of phosphorus into the inorganic framework of mesoporous TiO_2 from H_3PO_4 can inhibit the grain growth and stabilize the mesoporous structure of TiO_2. The study of Gao et al. [38] showed that $NH_4H_2PO_4$ doped TiO_2 had an improved activity in photocatalytic decom-

* Corresponding author. Tel.: +86 22 27892143; fax: +86 22 27892143.
E-mail address: zhyjiang@tju.edu.cn (Z. Jiang).

1381-1177/$ – see front matter © 2006 Elsevier B.V. All rights reserved.
doi:10.1016/j.molcatb.2006.06.005

position of hexane in air stream under the UV light irradiation. To the best of our knowledge, it has not been reported for the photocatalytic property of phosphorus doped TiO_2 nanomaterials in the visible-light region until now.

In the previous work [40], we found that carbon-containing TiO_2 nanoparticles prepared by the sol–gel method, together with $[Cp^*Rh(bpy)(H_2O)]^{2+}$ as the electron mediator, can catalyze the photoregeneration of NADH under the visible-light irradiation. However, this process remains to look for other photocatalysts with more efficient catalytic activity and more solar energy utilization. In the present work, the textural, optical and photocatalytic properties of P-doped TiO_2 prepared by the sol–gel method have been studied. It is observed that the doping of phosphorus can narrow the band gap of TiO_2, and photocatalytically regenerate NADH under visible-light irradiation.

2. Experimental

2.1. Materials

NAD^+ and NADH were purchased from Sigma. $[Cp^*Rh(bpy)Cl]Cl$ was synthesized according to the literature methods [41], which can readily hydrolyze to $[Cp^*Rh(bpy)(H_2O)]^{2+}$ in water. All the other reagents were of analytic grade and the water used was deionized.

2.1.1. Preparation of P-doped TiO_2 nanoparticles

P-doped TiO_2 nanoparticles were prepared by a sol–gel process. In a typical experiment, 6.8 g tetra-*n*-butyl titanium (as the precursor of TiO_2) was dissolved in 20 ml absolute ethanol. And then, the mixture including 4.0 ml deionized water, 20.0 ml ethanol, 4.0 g acetic acid and a certain quality of NaH_2PO_4 (as the precursor of P) were added dropwise at room temperature. During this process, the whole solution was stirred magnetically until gels formation. After aged at −10 °C for 72 h and lyophilized for 0.5 h, these samples were calcined at 480 °C for 8 h. and the sample of TiO_2 coupled with 2–6 mol% phosphorus was obtained. Unmodified TiO_2 were prepared as the same sol–gel process without NaH_2PO_4.

2.1.2. Characterization of P-doped TiO_2 nanoparticles

The X-ray power diffraction (XRD) patterns were recorded on a Philips X'Pertpro diffractometer using Co Kα radiation to determine the crystallite size and identity with 40 kV of accelerating voltage and 40 mA of applied current. The scanning electron microscopy (SEM) observation was committed on a Philips XL-30 SEM. The Brunaure–Emmett–Teller (BET) surface area (S_{BET}) was determined by using a ThermoFinnigan Sorptomatic1990 nitrogen adsorption apparatus. The UV–vis spectra of TiO_2 samples were obtained by using a Perkin-Elmer Lambda35 UV–vis spectrophotometer. The surface property of TiO_2 samples was characterized by X-ray photoelectron spectroscopy (XPS) in a Perkin-Elmer PHI 1600 ESCA system with a monochromatic Mg Kα source and a charge neutralizer.

2.1.3. Photogeneration of NADH

The regeneration of NADH photocatalyzed by the P-doped TiO_2 nanoparticles was carried out at 37 °C using a water-cooled cylindrical 100 ml quartz reactor. The weight of catalyst powder used in each experiment was kept at 80 mg. Prior to experimentation, the solution of NAD^+ and $[Cp^*Rh(bpy)(H_2O)]^{2+}$ was allowed to reach adsorption equilibrium with the photocatalyst in the reactor. The initial concentrations of NAD^+ and $[Cp^*Rh(bpy)(H_2O)]^{2+}$ after the adsorption equilibrium were 0.2 mmol/l. When an 8 W daylight lamp ($\lambda > 400$ nm) above the reactor was turned on, the experiment started. At a certain interval, the concentration of NADH produced in the photocatalytic reaction was determined by UV–vis spectrophotometer (Hitachi U-2800) at 340 nm and the NAD^+/NADH ratio in the reaction mixture was determined by HPLC (Agilent 1100 series system) with a ZORBAX-C_{18} gel column (4.6 mm × 250 mm, Agilent). HPLC conditions were as below: the mobile phase was 0.2 mol/l sodium phosphate buffer (pH 6.5)/methanol (9:1); the flowing rate was 0.5 ml/min; the temperature was 30 °C; the monitor wavelength was at 254 nm; the retention times of NAD^+ and NADH were 5.9 and 6.8 min, respectively.

3. Results and discussion

3.1. Characterization of P-doped TiO_2 nanoparticles

The effect of phosphorus doping amount on the optical and photocatalytic properties of TiO_2 nanoparticles was investigated. Fig. 1 shows the XRD spectra of 0, 2, 4 and 6 mol% P-doped TiO_2 nanoparticles after calcinations at 480 °C for 8 h. It reveals that the crystal phase of TiO_2 is only anatase present in all samples but the peaks in three P-TiO_2 samples become wider than that of the control sample, indicating that the size of TiO_2 turns smaller after doping with phosphorus. Since more evidences suggest that anatase is more active than rutile for oxidative detoxification reactions recently [42], the effect of

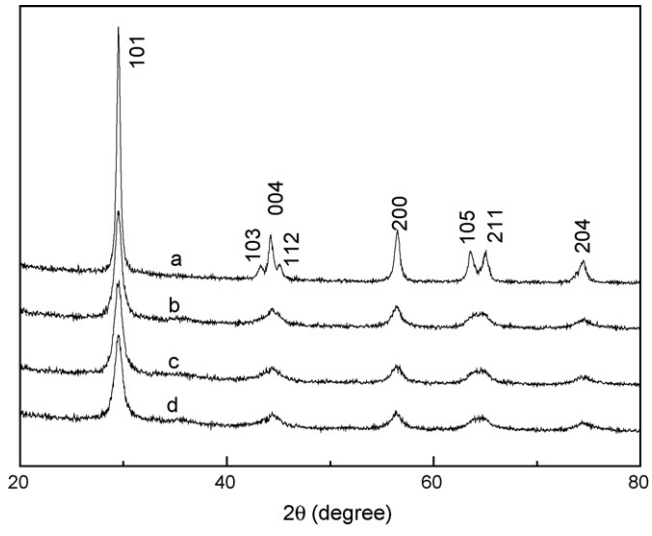

Fig. 1. XRD patterns of TiO_2 nanomaterials: (a) pure anatase TiO_2; (b) 2%-P-doped TiO_2; (c) 4%-P-doped TiO_2; (d) 6%-P-doped TiO_2.

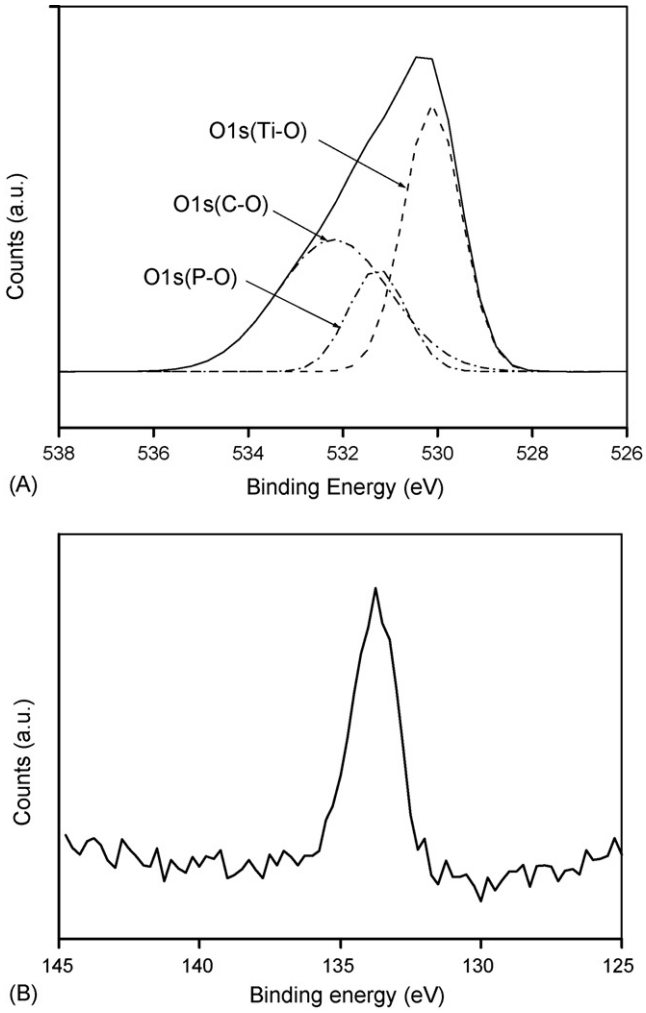

Fig. 2. XPS spectra of the O 1s (A) and P 2p (B) region taken on the surface of 6%-P-doped TiO_2 nanoparticles.

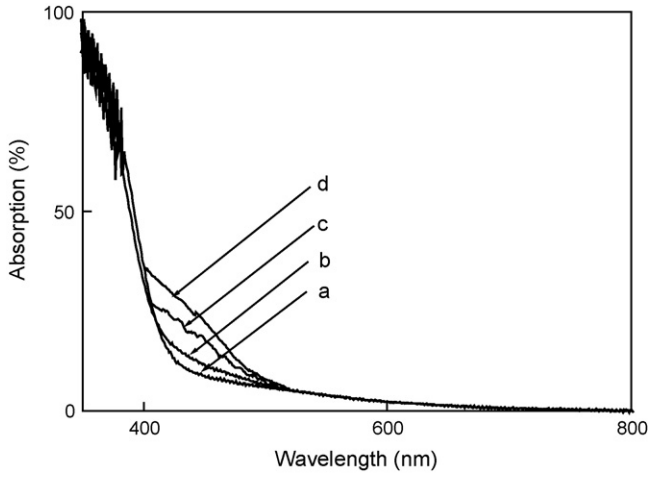

Fig. 3. UV–vis spectra of TiO_2 nanomaterials: (a) pure TiO_2; (b) 2%-P-doped TiO_2; (c) 4%-P-doped TiO_2; (d) 6%-P-doped TiO_2.

phosphorus doping on the properties of rutile was not investigated herein. According to the line width analysis of the anatase (1 0 1) diffraction peak based on the Scherrer formula [43], the averaged crystallite sizes of four TiO_2 samples are estimated to be about 43, 21, 15 and 14 nm with the increase of doped phosphorus amount from 0 to 6 mol%. Accordingly, the BET specific surface areas of the as-prepared samples increased from 31.1 m^2/g of pure TiO_2 to 68.4 m^2/g of 6%-P-doped TiO_2, with the decrease of crystallite sizes. Based on the result of Yu et al. [37], P-doping could inhibit the growth of anatase grains during calcination, leading to the decrease of TiO_2 nanoparticles in size. However, because of the agglomeration in calcination process, SEM photos (data not shown) show that the materials become lump about several micrometers in diameter.

Fig. 2 shows the X-ray photoelectron spectroscopy (XPS) measurements of O 1s and P 2p taken on the surface of 6%-P-doped sample. Seen from Fig. 2A, the O 1s region of 6%-P-doped TiO_2 nanoparticles can be fitted by three peaks, including Ti–O bonds, P–O bonds and C–O bonds, respectively. For phosphorus doped in the TiO_2, there is only one peak at 134 eV in the P 2p XPS spectrum (Fig. 2B), indicating that P ions are in the pentavalent-oxidation state (P^{5+}). It is unlikely that Ti–P bonds are present in the P-doped TiO_2 since the characteristic peak of P in TiP at 129 eV was not observed. Thus, it is evaluated that the P^{5+} replaced a part of Ti^{4+} in the crystal lattice of TiO_2, which resulted in the charge imbalance [44] and decreased the recombination rate of photogenerated electrons and holes. However, the nature of interaction between P and TiO_2 is not quite clear presently, which remains a problem worthy of further research.

UV–vis spectra were measured to investigate the optical response of P-doped TiO_2 nanoparticles. As shown in Fig. 3, phosphorus doping obviously affects light absorption characteristics of TiO_2. Unmodified TiO_2 nanoparticles hardly absorb visible light, while P-doped TiO_2 nanomaterials have a new absorption band at around 450 nm as a shoulder peak, suggesting the formation of an impurity energy level within the band gap. Moreover, the absorption in this range increases with the increase of doped phosphorus content. This clearly indicates a decrease of the band gap energy of TiO_2, although no shift in the absorption edge appears. Generally, the rate of the photocatalytic reaction is proportional to $(I_\alpha \Phi)^n$ ($n = 1$ for low light intensity and $n = 1/2$ for high light intensity), where I_α is the photo number absorbed by photocatalyst per second and Φ is the efficiency of the band gap transition [29]. Phosphorus doping can extend the wavelength response range to the visible region and increase the number of photogenerated electrons and holes to participate in the photocatalytic reaction, which would enhance the photocatalytic activity of TiO_2.

3.2. Photocatalytic activity studies

The photocatalytic activity of TiO_2 samples is evaluated by measuring the photoregeneration of NADH with $[Cp^*Rh(bpy)(H_2O)]^{2+}$ as the electron mediator and H_2O as the electron donor. Fig. 4 illustrates the regeneration of NADH photocatalyzed by P-doped TiO_2 as a function of illumination time. It can be observed that the regeneration of NADH reaches equilibrium after 9 h of irradiation, and P-doping could obviously enhance the photocatalytic activity of nanosized TiO_2 particles

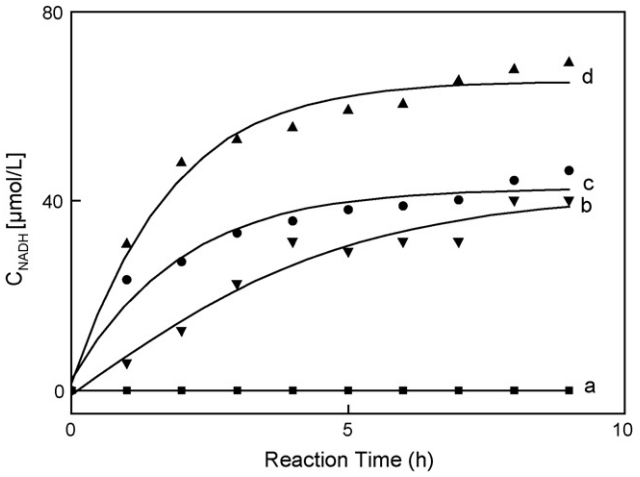

Fig. 4. Photoregeneration of NADH catalyzed by P-doped TiO_2 as a function of illumination time with different molar ratios of P to Ti: (a) pure TiO_2; (b) 2%-P-doped TiO_2; (c) 4%-P-doped TiO_2; (d) 6%-P-doped TiO_2.

under visible-light illumination. Moreover, the photoregeneration rate of NADH increased with the increase of phosphorus amount. When the molar ratio of P to Ti is 6%, the TiO_2 nanoparticle can photocatalytically reproduce 34.6% NADH under visible light, however, pure TiO_2 shows quite low photocatalytic activity under visible-light irradiation. The enlargement of photocatalytic ability can be attributed to the enhanced surface area and narrowed band gap of TiO_2.

3.3. Possible model of electron transfer pathway

One possible explanation for this photocatalytic activity enhancement of P-doped TiO_2 is that the phosphorus doping can result in the formation of charge carrier traps on the surface of TiO_2, suppressing recombination of the separated electron and hole and narrowing the band gap of TiO_2. Concretely, the electrons excited from the valence band (VB) by visible light injected into the surface traps (ST) arising from P doping, instead of the conduction band (CB) of titanium dioxide as shown in Scheme 1. And then, the $[Cp^*Rh(bpy)(H_2O)]^{2+}$ absorbed on the semi-conductor surface captured them to convert into $[Cp^*Rh(bpy)H]^+$. Subsequently, the transformation of NAD^+ to NADH can be achieved by the oxidation process of $[Cp^*Rh(bpy)H]^+$ to $[Cp^*Rh(bpy)(H_2O)]^{2+}$. On the other hand, holes on the surface of TiO_2 can regain electrons in the oxidation of electron donor.

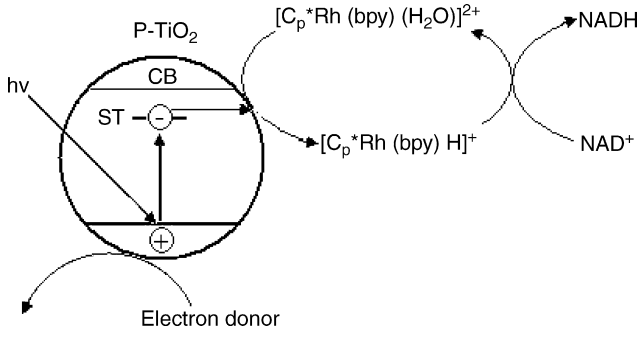

Scheme 1. Cartoon illustrating the electron transfer pathway in the photoregeneration system of NADH with P-doped TiO_2 as the photocatalyst and $[Cp^*Rh(bpy)(H_2O)]^{2+}$ as the electron mediator, in which CB, VB and ST are the abbreviations of conduction band, valence band and surface trap, respectively.

The photoregeneration rate of NADH is relative low using H_2O as the electron donor, because the ability of H_2O to provide electrons is relatively weak. To improve the photocatalytic activity of the TiO_2 nanomaterials doped with phosphorus, the study of other strong electron donors, such as mercaptoethanol, ascorbic acid and EDTA, etc., is in progress. In addition, NADH and NAD^+ could also be the electron donor oxidized by photo excited holes, which is another reason resulting in the low regeneration rate of NADH. The detailed mechanism is still being investigated.

4. Conclusions

In summary, it has been demonstrated that the presence of phosphorus can efficiently inhibit the grain growth and increase the surface area of TiO_2 nanomaterials. Based on XPS images and UV–vis spectra, it was speculated that the phosphorus doping enhance the absorption ability of TiO_2 nanoparticles in the visible light range and decrease the recombination of photogenerated electrons and holes because P^{5+} can accept photoelectron as the electron trap center. Moreover, the coupled semiconductor materials show relative high photocatalytic activity in the photoregeneration reaction of NADH under visible-light irradiation. This study would provide an easy pathway for the production of environmentally benign photocatalyst with relative efficient visible-light photocatalytic activity. Investigation is being carried out to dope other additives such as porphyrin, to improve the visible-light absorption and photocatalytic activity of these P-doped TiO_2 nanomaterials.

Acknowledgements

This work is supported by Program for Changjiang Scholars and Innovative Research Teams in University (PCSIRT). We would like to thank Professor Zhong Shunhe and Professor He Fei for their kind assistance in Diffuse Reflectance Spectra and XPS measurement, respectively.

References

[1] K.M. Koeller, C.-H. Wong, Nature 409 (2001) 232.
[2] A. Schmid, J.S. Dordick, B. Hauer, A. Kiener, M. Wubbolts, B. Witholt, Nature 409 (2001) 258.
[3] H. Zhao, W.A. Donk, Curr. Opin. Biotech. 14 (2003) 583.
[4] W.A. Donk, H. Zhao, Curr. Opin. Biotech. 14 (2003) 421.
[5] N. St. Clair, Y.F. Wang, A.L. Margolin, Angew. Chem. Int. Ed. 39 (2000) 380.
[6] J.M. Vrtis, A.K. White, W.W. Metcalf, W.A. Donk, J. Am. Chem. Soc. 123 (2001) 2672.
[7] J.M. Vrtis, A.K. White, W.W. Metcalf, W.A. Donk, Angew. Chem. Int. Ed. 41 (2002) 3257.
[8] T. Endo, S. Koizumi, Adv. Synth. Catal. 343 (2001) 521.
[9] N. Itoh, M. Matsuda, M. Mabuchi, T. Dairi, J. Wang, Eur. J. Biochem. 269 (2002) 2394.

[10] W.A. Duetz, J.B. Beilen, B. Witholt, Curr. Opin. Biotechnol. 12 (2001) 419.
[11] F. Hollmann, A. Schmid, E. Steckhan, Angew. Chem. Int. Ed. 40 (2001) 169.
[12] F. Hollmann, B. Witholt, A. Schmid, J. Mol. Catal. B: Enzym. 19–20 (2002) 167.
[13] P.S. Wagenknecht, J.M. Penney, R.T. Hembre, Organmetallics 22 (2003) 1180.
[14] D. Mandler, I. Willner, J. Am. Chem. Soc. 106 (1984) 5352.
[15] D. Mandler, I. Willner, J. Chem. Soc., Perkin Trans. 2 (1986) 805.
[16] Z. Goren, N. Lapidot, I. Willner, J. Mol. Catal. 47 (1988) 21.
[17] I.A. Shumilin, V.V. Nikandrov, V.O. Popov, FEBS Lett. 306 (1992) 125.
[18] T. Itoh, H. Asada, K. Tobioka, Bioconj. Chem. 11 (2000) 8.
[19] H. Asada, T. Itoh, Y. Kodera, Biotechnol. Bioeng. 76 (2001) 86.
[20] M.R. Hoffmann, S.T. Martin, W. Choi, D.W. Bahnemann, Chem. Rev. 95 (1995) 69.
[21] M.A. Fox, M.T. Dulay, Chem. Rev. 93 (1993) 341.
[22] M. Anpo, M. Takeuchi, J. Catal. 216 (2003) 505.
[23] C. Chen, X. Li, W. Ma, J. Zhao, J. Phys. Chem. B 106 (2002) 318.
[24] H. Einaga, M. Harada, S. Futamura, T. Ibusuki, J. Phys. Chem. B 107 (2003) 9290.
[25] Y. Xie, C. Yuan, Appl. Catal. B: Environ. 46 (2003) 251.
[26] C.T.K. Thaminimulla, T. Takata, M. Hara, J.N. Kondo, K. Domen, J. Catal. 196 (2000) 362.
[27] R. Asahi, T. Morikawa, T. Ohwahi, K. Aoki, Y. Taga, Science 293 (2001) 269.
[28] C. Burda, Y. Lou, X. Chen, A.C.S. Samia, J. Stout, J.L. Gole, Nano Lett. 3 (2003) 1049.
[29] J.C. Yu, J. Yu, W. Ho, Z. Jiang, L. Zhang, Chem. Mater. 14 (2002) 3808.
[30] R. Gómez, T. López, E. Ortiz-Islas, J. Navarrete, E. Sánchez, F. Tzompanztzi, X. Bokhimi, J. Mol. Catal. A: Chem. 193 (2003) 217.
[31] A. Kumar, A.K. Jain, J. Mol. Catal. A: Chem. 165 (2001) 265.
[32] M.H. Bartl, S.W. Boettcher, K.L. Frindell, G.D. Stucky, Acc. Chem. Res. 38 (2005) 263.
[33] M.H. Bartl, S.P. Puls, J. Tang, H.C. Lichtenegger, G.D. Stucky, Angew. Chem. Int. Ed. 43 (2004) 3037.
[34] M. Gärtner, V. Dremor, P. Müller, H. Kish, Chemphyschem 6 (2005) 1.
[35] T.M.R. Viseu, G. Hungerford, M.I.C. Ferreira, J. Phys. Chem. B 106 (2002) 1853.
[36] W.M. Campbell, A.K. Burrell, D.L. Officer, K.W. Jolley, Coordin. Chem. Rev. 248 (2004) 817.
[37] J.C. Yu, L. Zhang, Z. Zheng, J. Zhao, Chem. Mater. 15 (2003) 2280.
[38] B.H. Cai, X.P. Zhao, Y.H. Yue, Z. Gao, J. Mol. Catal. (China) 17 (2003) 302.
[39] B.H. Cai, X.N. Ye, Y.H. Yue, Z. Gao, J. Mol. Catal. (China) 18 (2004) 136.
[40] Z. Jiang, C. Lü, H. Wu, Ind. Eng. Chem. Res. 44 (2005) 4165.
[41] F. Hollmann, B. Witholt, A. Schmid, J. Mol. Catal. B: Enzym. 19–20 (2003) 167.
[42] T. Berger, M. Sterter, O. Diwald, E. Knözinger, D. Panayotov, T.L. Thompson, J.T. Yates, J. Phys. Chem. B 109 (2005) 6061.
[43] Scherrer formula: $L = K\lambda/\beta\cos\theta$, L is the crystalline size in nm; λ (0.151 nm) the wavelength of the X-ray radiation; K is usually taken as 0.89; β the line width at half-maximum height after subtraction of equipment broadening at the peak of 25.3°.
[44] J.C. Yu, W. Ho, J. Yu, H. Yip, P.K. Wong, J. Zhao, Environ. Sci. Technol. 39 (2005) 1175.